Identification of Composite Insulator Criticality based on a new Leakage Current Diagnostic Index

M. F. Palangar, U. Amin, H. Bakhshayesh, G. Ahmad, A. Abu-Siada, M. Mirzaie

***Abstract*—In this paper, a new method is proposed to identify the health condition of composite insulators through investigating the leakage current (LC) along with the electric potential (EP) and electric field stress (EFS) profiles. In this regard, variations of the LC harmonics and the distribution profiles of the EP and EFS are investigated through series of experimental and simulation analyses conducted on composite insulators under various environmental and pollution conditions. Fast Fourier Transform and COMSOL-Multiphysics environment are utilized to analyze this variation. Results reveal a strong correlation between the LC harmonics and the insulator health condition. A new diagnostic criticality index based on the third to the fifth harmonic ratio of the insulator LC is proposed to quantify the composite insulator criticality and predict the likelihood of flashover occurrence. The EP and EFS analysis can be used to provide a complimentary diagnosis to the insulator health state under severe pollution and humidity conditions. The proposed analysis enables the transmission line network operator to get an insight into the insulators' functional status and thus improving the network reliability through avoiding insulator failure and adopting a proper condition-based maintenance scheme.**

***Index Terms*— Composite insulator, condition monitoring, leakage current, electric field distribution, flashover.**

I. Introduction

Overhead line insulator represents a key component in transmission and distribution networks as it provides insulation and mechanical support to the power lines. Because they are operating under harsh environmental conditions, overhead insulators are subjected to aging deterioration due to the effect of pollution and humidity [1]. Humidity and pollution on the surface of the insulators increase the likelihood of leakage current (LC) flow through the insulator surface, which may result in a flashover arc [2]. As such, recent studies focused on the development of various methods to detect incipient LC flow on a polluted insulator string [3-7]. Although the LC peak value can be used as an indicator, it is not reliable since it can't be correlated to the waveform structure accurately [3]. Fiber-optic and electromagnetic current sensors, directly connected to one insulator of the string, are used to detect the LC and eliminate the effect of electromagnetic interference on the measured signal [4, 5]. This system is capable to monitor and characterize the main features of the LC. Likewise, in [6, 7] LC measurement sensor is constructed using a single light-emitting diode coupled with an optical fiber. In these studies, processing modules are developed to detect, store and classify the peaks of the LC that are directly related to partial discharges on the surface of the high voltage insulators. In [8], a method is presented to reveal the insulator's state using an electro-optic E-field sensor that can detect conductive defects of high voltage composite insulators. While the use of sensors technology to detect insulators LC has been presented in several papers in the literature, further investigations are still required to validate the practical feasibility of this technology, in particular for insulators operating under wet and polluted conditions.

In several studies, the LC is used as a criterion to assess the condition of the insulators and provide an early warning signal for the likelihood of flashover occurrence. In [9] the magnetic field around the dry band is proposed as a criterion to detect the critical condition of the insulator. In this study, dry band formation is investigated through insulator surface resistivity and LC measurement by varying the pollution level on the insulator surface using different salt mixtures. Reported results indicate that the dry band formation is non-uniform with different salt mixtures and the magnitude of the electric field increases in the dry band region. In [10, 11] LC of composite insulators is analyzed with different contamination and hydrophobic state. It is found that under the same voltage, the amplitude of LC is directly correlated with the equivalent salt deposit density on contaminated insulators. Similarly, in [12] composite insulators' LC behavior is studied using the recurrence plot method. This method utilizes a signal processing technique to convert the electrical signal into a 2D representation for visual analysis. In [13] interfacial performance of the core and sheath of composite insulators is evaluated by the LC to identify the aging condition and inner defects.

In other studies, along with the insulator state detection by the LC analysis, the probability of flashover occurrence is discussed. In [14-16], the phase angle difference of the applied voltage and LC is analyzed to predict the insulator's state and the likelihood of flashover occurrence. In [17], an analysis of the LC harmonics components is presented to identify the

Manuscript received on X Month, 2021, in final form XX Month, 2021.

M. F. Palangar is with the Department of Electrical Engineering, Flinders University, Adelaide 5042, Australia.
U. Amin, H. Bakhshayesh and A. Abu-Siada are with the School of Elec Eng, Comp and Math Sci, Curtin University, Perth 6102, Australia.
G. Ahmad is with the School of Electrical Engineering, Southeast University, Nanjing, China.
M. Mirzaie is with the School of Electrical and Computer Engineering, Babol University of Technology, Babol, Iran.

condition of the insulator. In this study, the LC is measured within various critical range conditions in which the probability of flashover occurrence is high. In [18], harmonic components of the LC signal on composite insulators are analyzed to predict flashover occurrence. The study considered the LC total harmonic distortion (THD) as a criterion to identify the condition of the insulator. Further, the probability of flashover occurrence is calculated through a geometric probability distribution.

While some of the published papers in the literature proposed various numerical indices to identify the state of insulators, none of them evaluated the performance of such indices on the insulators of overhead lines. Only acoustic and thermal-based diagnostic methods such as infrared thermal imaging [19], ultrasonic wave [20], acoustic fault diagnosis [21], wireless-based system [22], instance segmentation and temperature analysis of infrared insulator images [23], visible light images [24], artificial neural network (ANN)-based methods [25], network sensors [26] and long-term analysis of LC using optical sensor [27] have been used to evaluate the health condition of the overhead line insulator in real-time.

Despite the LC features being the most effective tool to identify the health condition of the insulators as reported in the literature, its feasibility for real-time applications has not been explored yet [20]. A deep learning neural network model based on aerial images to identify the insulator criticality was recently presented in [28]. A hardware detector to monitor the insulators' state using a combination of two LC harmonic ratios and phase angles is presented in [29]. Though most of the above studies offer useful methods to detect the condition of different types of insulators, little research is conducted to predict the probability of flashover occurrence, specifically for composite insulators. Furthermore, not much attention was given to establish a correlation between the insulator critical condition and the electric field distribution profile over its surface. Also, a proper and widely accepted method to quantify the probability of flashover occurrence has not been presented yet.

This paper is taking one step forward into filling this research gap by proposing a new insulator criticality index to properly identify the composite insulator health state and quantify the probability of flashover occurrence. Furthermore, analysis of the electric potential (EP) and electric field stress (EFS) distribution profiles is proposed to provide a complimentary diagnosis to the insulator health state under severe pollution and humidity conditions. Fig. 1 summarizes the paper's motivation, contribution, and advantages of the proposed method. Table I lists various insulator diagnostic methods that are not using LC harmonic components characteristics along with the disadvantage of each method. In all these methods, the index declaring the insulator's state is based on the physical aspects of the insulator while the LC characteristic refers to the inherent features of the insulator [2, 14-17]. LC characteristics comprise several numerical indices such as amplitude, total harmonic distortion, frequency, harmonic components, and phase angle. There is a strong correlation between harmonic components and phase angle variations and the insulator's state. Also, LC measurement and its analysis are easier than other methods as elaborated in Table I.

TABLE I
COMPARISON OF THE INSULATOR STATE DIAGNOSTIC METHODS

Ref.	Diagnostic Method	Disadvantages
[4]	An optical sampling of LC	Costly and calls for expert personnel.
[14-16]	Phase angle difference between voltage & LC	Hard to record applied voltage on an insulator in real overhead lines
[19, 23, 24]	The infrared thermal image camera	Relies on the thermal features of the insulator, which cannot reveal the accurate condition of the insulator.
[20, 21]	Ultrasonic waves acoustic fault diagnosis	Performance is affected by the acoustic frequency noise resulting from the line's electromagnetic field.
[25]	ANN-based near-field microwave technique	Affected by electric and magnetic fields.
[26]	Aerial images	Not an accurate index since it relies on image processing of the pollution layers on the insulator surface.

II. EXPERIMENT AND SIMULATION ANALYSIS

A. Lab Setup

A laboratory setup as shown in the schematic of Fig. 2 is used to conduct series of insulators testing under various pollution conditions. This setup is built according to the IEC60507 standard for artificial pollution tests on high-voltage insulators [16]. The setup comprises a clean fog chamber, high voltage transformer, and LC measuring system. A capacitive voltage divider is used to measure the voltage applied to the insulator. The LC signal is captured using a digital oscilloscope and the data are stored as CSV files and are analyzed using MATLAB software. The LC meters along with the oscilloscope are protected against overcurrent and surge voltages.

B. Studied Insulators

Two composite insulators of different voltTaage ratings (11 kV and 33 kV) are used to investigate the ability of the proposed technique to detect their critical conditions. Detailed specifications of the two insulators are listed in Table II. The composite insulator consists of a metal fitting at both ends usually made of forged steel and a fiber-reinforced plastic core as a load-bearing structure, where silicon rubber is used for sheds and sheath due to its hydrophobic nature. The selected insulators are tested under different artificial pollution levels proposed by the IEC 60507 standard. Fig. 3 shows a 2D schematic of the two investigated insulators, developed using COMSOL Multiphysics simulation software. It is worth mentioning that, five different composite insulators have been tested under various pollution conditions, humidity, and voltage levels. The LC signal was recorded and analyzed for each test. Results of the tested insulators are comparable which verifies the robustness of the proposed diagnostic method. Sample results of only two particular insulators are presented in this paper as they are the most employed insulator types in distribution overhead lines.

Contributions

1- An extensive set of experimental tests conducted under various environmental conditions (i.e., pollution and humidity) to collect a rich set of experimental data of the targeted indicator.
2- Computer-aided analysis to analyse insulator's electric field stress variations.
3- Simultaneous consideration of two factors (3rd to 5th harmonic ratio and EFS) to get the highest level of precision and reliability in insulator's state detection.

Advantages

1- Monitoring insulators state on overhead power lines using the proposed indicator in real-time.
2- Declaring insulators state according to LC characteristics (the most accurate factors).
3- Applicable for any types of insulators.
4- Possibility to Prototype an automatic detector device based on the determined reference values of the proposed factors ($R_{3/5}$% and EFS) to diagnose the overhead lines insulator state.

Fig. 1. Contributions, and advantages of the proposed method

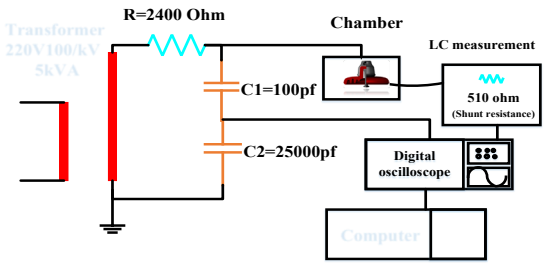

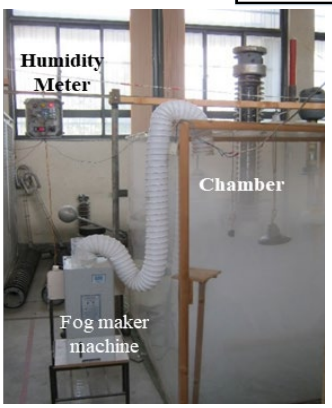

Fig. 2. Schematic and real image for the experimental setup.

TABLE II
CHARACTERISTICS OF INSULATORS UNDER TEST

Characteristics	#1	#2
Nominal Voltage, kV	33	11
Spacing (*H*), mm	720	318
Creepage distance (*L*), mm	1070	525
Shed diameter (*D*), mm	100/86	134/105
Electromechanical Failing load, kN	70	70

C. Polluting the Insulator

To pollute the insulator surface, the solid layer method following the IEC60507 standard is used. The standardized pollution levels are divided into four categories; light, medium, heavy, and very heavy. To create pollution at different levels, salt with 40 grams of kaolin is dissolved in 1000 ml of water. The amount of salt has a direct effect on the electrical conductivity of the solution. Table III shows the amount of salt dissolved in 1 liter of distilled water and the corresponding

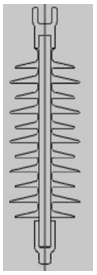

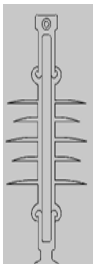

Insulator #1 Insulator #2

Fig. 3. 2D Schematic view of the two insulators under study.

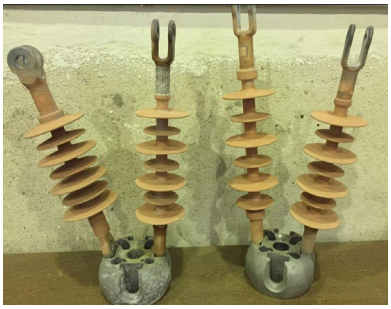

Fig. 4. Sample of polluted composite insulators.

TABLE III
SALT CONCENTRATION AND CORRESPONDING POLLUTION LEVEL

Pollution level	Light	Medium	Heavy	Very heavy
Salinity (g/litre)	10-20	20-40	40-80	80-100

pollution intensity. Fig. 4 shows a sample of the polluted composite insulators used in the experimental measurements. Fig. 5 shows schematic view of different pollution levels simulated on insulator #2 as a sample of the obtained results (similar analysis is conducted on insulator #1).

D. Simulation Modeling

In addition to the experimental testing, COMSOL software is used to simulate both composite insulators considering three different levels of uniform pollution layers of 0.5, 1.5-, and 3-mm thickness on the insulator surface. Input parameters for the COMSOL Multiphysics software include the physical geometrical dimensions of the insulator, material permittivity, and conductivity along with the boundary conditions such as the potential of metal parts. The relative permittivity and electric conductivity of each material used in this study are listed in Table IV. To investigate the effect of humidity on the insulator LC waveform, water droplets are modeled on the insulator shed and shank. The investigated insulator is simulated under two cases: water droplets on a clean insulator surface and water droplets on a uniformly polluted surface as shown in Figs. 6a and 6b; respectively. Each drop is modeled with a 3.0 mm diameter and a 90° contact angle with the insulator surface.

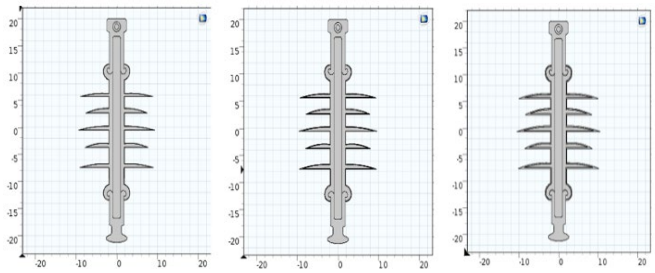

Fig. 5. 2D view for insulator #2 under three uniform pollution levels.

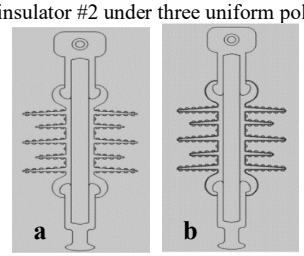

Fig. 6. Simulation of insulator #2 with water droplets on (a) clean surface and (b) polluted surface.

TABLE IV
CHARACTERISTICS OF THE MATERIALS USED IN THE SIMULATION

Material	Relative Permittivity, ϵ_r	Conductivity, (σ), S/m
Forged steel	1	5.9×10^{7}
Air Background	1	1×10^{-13}
Silicon rubber	4.3	1×10^{-12}
FRP core	7.2	1×10^{-12}
Pollution layer	7.1	6×10^{-7}
Water droplet	80	5.5×10^{-6}

III. EXPERIMENT AND SIMULATION RESULTS

A. Leakage Current Measurement

In the performed experimental testing, the LC signals are sampled and stored as CSV files by the digital oscilloscope. Collected data are analyzed in MATLAB software using fast Fourier transform (FFT) to identify the harmonic contents in each signal. Each insulator is tested under clean and polluted conditions. In the case of the clean condition, the insulators are energized using their nominal voltages (33 kV for insulator #1 and 11 kV for insulator #2) with ambient humidity of 64%. In polluted conditions, insulators are energized at the nominal 50 Hz sinusoidal AC voltage with various pollution and humidity levels. First, to observe the effect of different pollution levels on the insulators LC, experiments are performed at a constant humidity level. Figs. 7 and 8 show an example for the measured and analyzed LC signals for insulator #1 under the clean condition at ambient humidity and under various pollution conditions at 77% humidity level. On the other hand, the measured LC for insulator #2 at various humidity levels and constant pollution is shown in Fig. 9. Results of Figs. 7 and 8 reveal that polluted insulator influences the LC signal in terms of amplitude and THD. However, there is no consistent trend for these two parameters with the pollution extent. Harmonic spectra of the LC at different pollution levels indicate that the 3rd and 5th components dominate the harmonic spectrum. However, they cannot be used individually to quantify the pollution extent due to the lack of a consistent trend. As such, the ratio of these two components is proposed in this paper as a more reliable indicator to identify and quantify the insulator condition.

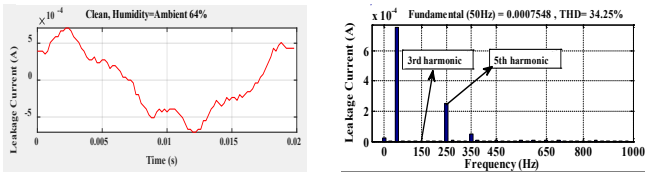

Fig. 7. Measured LC and FFT analysis for insulator #1 at ambient humidity (64%).

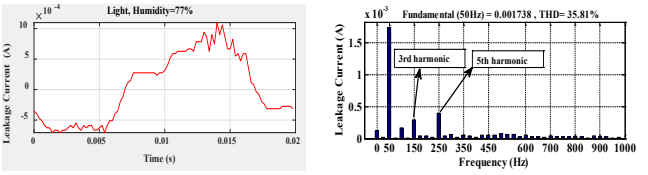

a. Light pollution

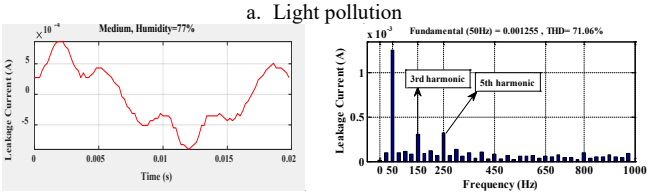

b. Medium pollution

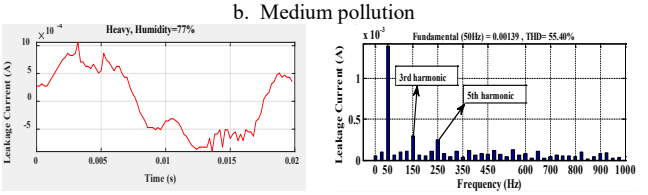

c. Heavy pollution

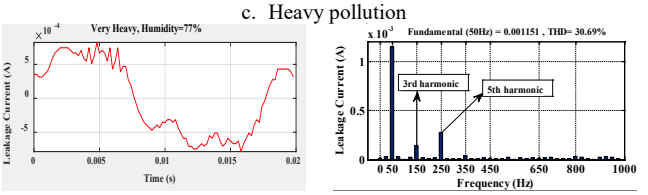

d. Very heavy pollution

Fig. 8. Measured LC and FFT analysis for insulator #1 at various pollution levels and constant humidity (77%).

Results of Fig. 9 indicate that by increasing the humidity level, assuming constant pollution condition, harmonic content in the LC signal is increasing and the LC signal is getting more distorted at high humidity levels in comparison with ambient humidity. Tables V and VI summarize the numerical values of the LC 3rd and 5th harmonic components for the investigated insulators under different humidity and pollution levels along with the clean insulator at 64% ambient humidity level.

Results show that with the presence of wet pollution on the insulator, the magnitude of the 3rd harmonic component increases remarkably compared with that measured for a clean insulator. When the wet pollution level increases, the magnitude of the 3rd harmonic component increases to a point, which goes beyond the magnitude of the 5th harmonic; at this stage electrical discharge is observed. These results indicate that the humidity level has a considerable impact on the LC 3rd harmonic component. However, it can be observed that in some cases and at high humidity level (91%), the surface electric conductivity decreases which put the insulators in an abnormal state instead of a critical state. This is because, at a high humidity level and due to the complete wetness of the insulator surface, the surface pollution may be washed out. This situation

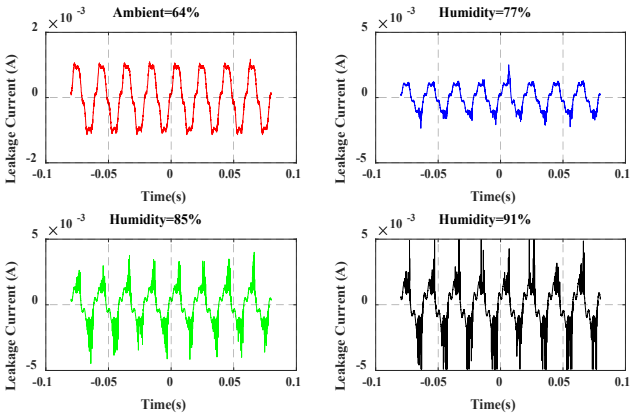

Fig. 9. Measured LC for insulator #2 at various humidity levels and constant pollution (heavy).

TABLE V
MAGNITUDE OF LC 3RD, 5TH HARMONICS AND $R_{3/5}$ % FOR INSULATOR #1

Humidity%	Severity pollution	3rdH (mA)	5thH (mA)	$R_{3/5}$%
Ambient 64%	clean	0.055	0.261	21.56%
77%	Light	0.14	0.143	97.79%
	Medium	0.176	0.324	54.46%
	Heavy	0.181	0.247	73.33%
	V. Heavy	0.029	0.313	9.3%
85%	Light	0.097	0.109	89.5%
	Medium	0.358	0.343	104.3%
	Heavy	0.084	0.18	46.73
	V. Heavy	0.234	0.179	130.7%
91%	Light	0.147	0.133	110.58%
	Medium	0.199	0.32	62.13%
	Heavy	0.188	0.173	108.6%
	V. Heavy	0.211	0.196	107.6%

TABLE VI
MAGNITUDE OF LC 3RD, 5TH HARMONICS AND $R_{3/5}$ % FOR INSULATOR #2

Humidity%	Severity pollution	3rdH (mA)	5thH (mA)	$R_{3/5}$%
Ambient 64%	clean	0.0044	0.242	1.7%
77%	Light	0.295	0.387	76.28%
	Medium	0.3	0.316	96.36%
	Heavy	0.295	0.247	119.3%
	V. Heavy	0.21	0.3	70.7%
85%	Light	0.204	0.298	68.42%
	Medium	0.229	0.201	113.9%
	Heavy	0.259	0.194	133.5%
	V. Heavy	0.264	0.228	115.7%
91%	Light	0.176	0.3	58.58%
	Medium	0.124	0.205	60.54%
	Heavy	0.239	0.339	70.7%
	V. Heavy	0.247	0.221	111.4%

can be observed in Table VI in which the $R_{3/5}$% for one case study is only 9.3% i.e. normal insulator condition although the pollution level is very heavy. In this case, the impact of pollution may have been reduced due to humidity level (77%) as explained above.

Fig. 10 shows the variations in the 3rd to 5th harmonic ratio ($R_{3/5}$%) versus solved salt (pollution level representative) and humidity for the two insulators under test. It can be seen that the proposed ratio increases with the increase in pollution and humidity levels. A summary of the insulator state based on the pollution and humidity levels using color coding is presented in

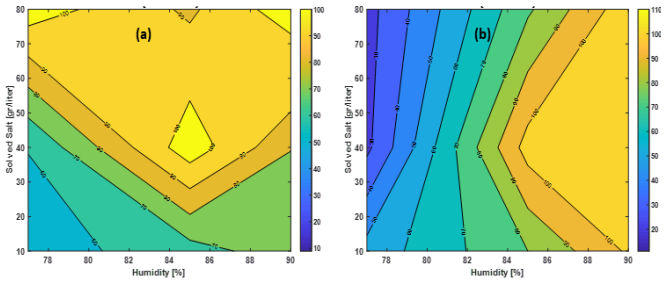

a. insulator #1 b. insulator #2

Fig. 10. $R_{3/5}$% variation versus pollution and humidity levels.

TABLE VII
INSULATOR OPERATIONAL MAP BASED ON POLLUTION AND HUMIDITY LEVELS

Condition	Color Code			
Normal				
Abnormal				
Critical				
Humidity / Pollution	64%	77%	85%	91%
Heavy				
Medium				
Light				
Clean				

Table VII. This table indicates that the insulator has a normal state in a dry condition for any level of pollution and also in a clean condition for any level of humidity.

B. *Electric Field Stress and Electric Potential*

Finite element analysis models are developed for the two investigated insulators using COMSOL software to analyze the electric field distribution over the insulator surface under different pollution and humidity levels. Simulation models are developed for three conditions; clean surface, the polluted surface without humidity, and polluted surface with humidity. The insulators are assumed to be polluted with a uniform pollution layer for a dry condition under which the EFS is calculated. The developed simulation models under different pollution and humidity levels are summarized in Table VIII. Obtained results are discussed below.

1) Clean Condition

Random surface partial arcs may be produced by the strong electric field surrounding water droplets on a polluted insulator. The thin polymer layer around the droplet is consumed by these arcs, removing its hydrophobicity. Under such conditions, water droplets come together to form filament which increases the field intensity and arcing over the insulator sheds. Wetted patches eventually produce a conducting route over the insulator sheds and result in the development of partial arcs which potentially lead to a surface flashover.

TABLE VIII
DEVELOPED SIMULATION MODELS UNDER DIFFERENT CONDITIONS

Conditions	Insulators 1# & #2
Clean surface	-----
Polluted surface without humidity	0.5, 1.5, 3 mm
Polluted surface with humidity	0.5mm, high humidity

Fig. 11 shows the electric field norm (kV/m) versus the arc length for insulators #1 and #2 under clean conditions. It can be seen that the two insulators are operating normally as the electric field distribution is within the normal range of 85 kV/m for insulator #1 and 55 kV/m for insulator #2. This can be attested from the surface electric field distribution of insulators # 1 and #2. In Fig. 12, the electric field distribution of under studied insulators is shown, which reveals normal EFD. Fig. 13 shows the EP variations for the two insulators versus the shed's arc length under clean conditions. It can be observed that the maximum EP mostly takes place at the shed's area close to the cap and pin while it decreases at the terminals of the sheds. Fig. 14 demonstrates the surface EP of under studied insulators in a clean condition. It can be seen that the maximum potential occurs at the point close to the power line while the minimum potential takes place at the point connected to the earthed tower.

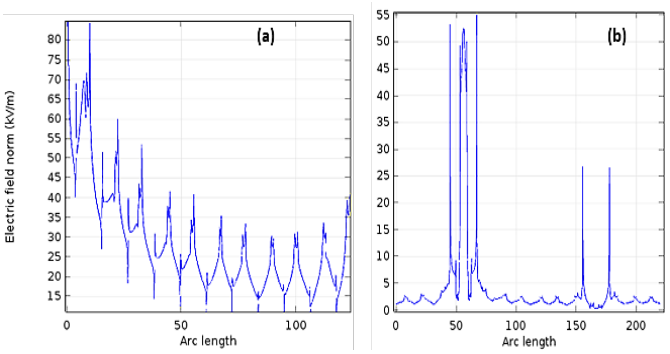

Fig. 11. Electric field stress profile under clean condition (a) insulator #1, (b) insulator #2.

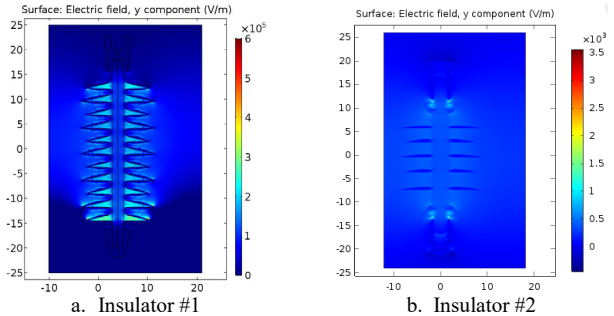

a. Insulator #1 b. Insulator #2

Fig. 12. Surface electric field of studied insulators under clean condition.

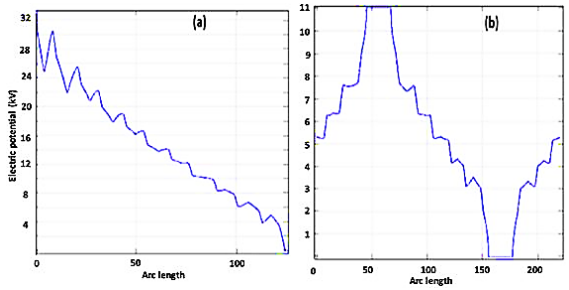

Fig. 13. Linear EP distribution of (a) insulator #1, (b) insulator #2.

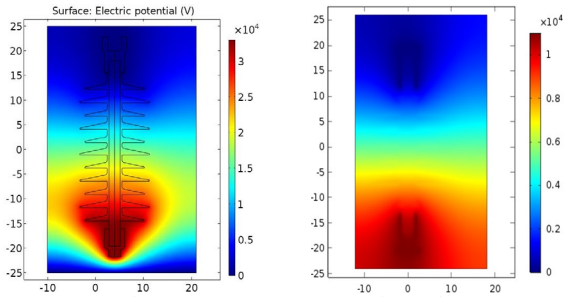

c. Insulator #1 d. Insulator #2

Fig. 14. Surface EP of studied insulators under clean condition.

2) Polluted Condition without Humidity

Both insulators are simulated for polluted conditions without humidity to investigate the effect of pollution layer thickness on the EFS. Figs. 15 and 16 show the results of insulators # 1 and # 2; respectively. Fig. 15(a) depicts the EFS of insulator # 1 when the surface is uniformly polluted with a pollution layer of 1.5 mm thickness. It can be seen that the maximum EFS of the insulator is 150 (kV/m). Fig. 15(b) shows that the surface EFS is maximum at the sheds close to the cap and pin of the insulator (similar analysis is studied for insulator #1 as well). Figs. 16(a) through (c) show the maximum electric field norm of insulator #2 with different pollution layer thicknesses of 0.5 mm, 1.5 mm, and 3 mm while keeping the pollution conductivity constant. As can be observed from these figures, the maximum electric field norm in the case of 0.5 mm pollution layer is 80 kV/m, which increases to 130 kV/m and 170 kV/m when the thickness of the pollution layer becomes 1.5 mm and 3 mm; respectively.

3) Polluted Condition with Humidity

Fig. 17 shows the maximum electric field norm when the surface of both insulators is uniformly polluted with a layer of 0.5mm thickness at a high humidity level. The maximum EFS of insulators #1 and #2 are 104 kV and 55 kV/m; respectively. In this case, due to the high level of humidity, the conductivity of the insulator surface is degraded which causes a reduction in the EFS. Simulation analysis is repeated with a pollution layer of 3 mm thickness at high humidity. Obtained results are reported in Table IX. It is to be noted that in dry pollution, the conductivity of the pollution layer is 0.6 µS/m and in wet pollution, the humidity is assumed in the medium range.

TABLE IX
MAXIMUM EFS OF INSULATORS IN A CLEAN AND POLLUTED ENVIRONMENT

Insulator No.	EFS (kV/m)		
	Clean	Dry Pollution (1.5 mm)	Wet Pollution (3 mm)
1	80	150	239
2	55	137	168

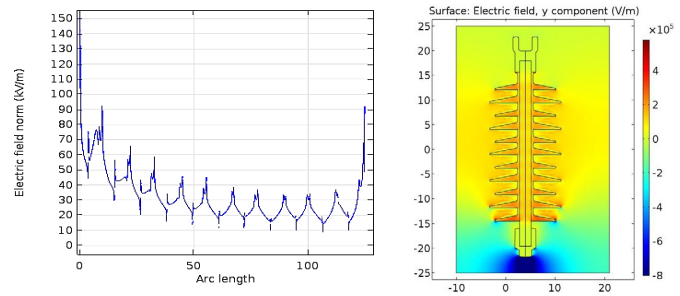

a. Electric field norm of insulator #1 vs. arc length.

b. Electric field distribution of insulator #1.

Fig. 15. Insulator #1 under uniformly polluted conditions (a) EFS, (b) Surface EFS.

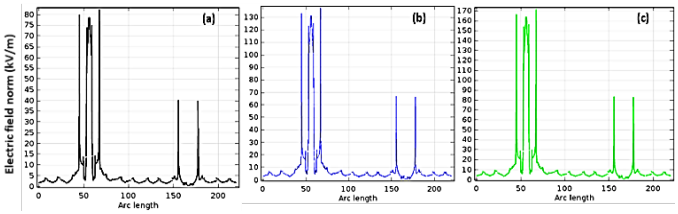

Fig. 16. Electric field stress of insulator #2 under uniformly polluted thicknesses (a) 0.5 mm (b) 1.5 mm (c) 3 mm.

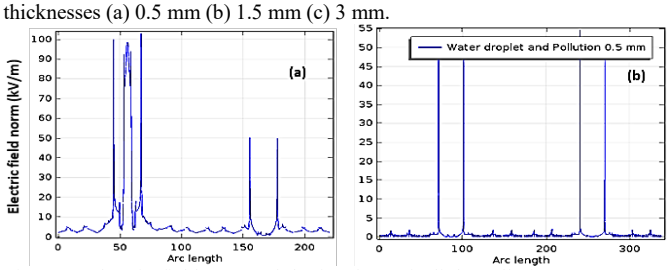

Fig. 17. Electric field stress of the insulators in light pollution (0.5mm) and humidity conditions (a) insulator #1, (b) insulator #2.

IV. Analysis And Discussions

In a clean state, no flashover is observed in any of the conducted experiments. Results indicate that the magnitude of the LC fundamental component increases considerably with the increase of the humidity level, which is not observed in other harmonic components. Also, it can be observed that under clean conditions, the 5th harmonic component of the LC signal is always higher than the magnitude of the 3rd harmonic component. Therefore, the insulator can be considered in normal condition if the ratio of the LC 3rd to the 5th harmonic components is less than one. For slightly polluted insulators, results indicate that the magnitude of the LC fundamental component encounters an inconsistent trend as it initially decreases but upon the presence of fog and humidity, it increases. After some time, it decreases and increases again at the starting of the humidity saturation region. It is observed that the most critical condition for insulators is the beginning of fog production on their surface. This is because the wetness of the insulator surface and dissolution of soluble salts cause a sudden increment in the insulator surface conduction. This increment in surface conduction along with the flow of the LC and the creation of dry bands eventually results in partial discharge on the insulator surface. In some tests, such partial discharge causes a sustained electrical arc on the insulator surface and flashover is visually observed. After a while of fog production and complete wetness of the insulator surface at a high humidity level, the pollution layer dissolves completely. Consequently, the solution appears as small droplets on the insulator surface and drips down the edges of the shed. This causes a further reduction of the salt and thus reduction of the surface conduction which results in a more stable operational condition of the insulator. Thus, it can be inferred that the probability of flashover occurrence in high humidity levels is very less if no flashover is observed at the beginning of the moistening region.

In the polluted insulators under no-fog conditions, the LC 5th harmonic component has always been more than the 3rd harmonic component. This indicates a normal status of the insulator. Thus, the previous criterion for the detection of normal working status in clean insulators is still applicable in polluted insulators. However, with the presence of fog and increased humidity, the magnitude of the 3rd harmonic component increases and gets larger than the 5th harmonic component. Although the 5th harmonic component also increases, the increase of the 3rd harmonic component prevails. Thus, the increment of the 3rd harmonic component with respect to the 5th harmonic component $R_{3/5}$% can be used to reveal the insulator condition. Obtained results indicate that when $R_{3/5}$% is less than 100%, the insulator is considered in normal condition whereas, for $R_{3/5}$%>100%, a critical insulator condition can be reported. The extent of criticality can be quantified through the value of $R_{3/5}$%. For instance, when the 3rd harmonic component of the LC is increased and the proposed index is in the range of 80%< $R_{3/5}$%< 100%, the insulator is considered abnormal. For $R_{3/5}$% greater than 100%, the probability of flashover occurrence is significantly high. This condition is essential but not sufficient to predict the flashover occurrence because, in some cases of $R_{3/5}$%>100%, the flashover may not take place.

Therefore, to further validate the feasibility of the proposed index and to accurately predict the probability of flashover occurrence in a polluted insulator, 54 experimental tests under different levels of pollution and humidity have been conducted. Results indicate that, in 34 cases out of 54, physical flashover has occurred. Out of these 34 cases, the proposed index was greater than 100% in 28 cases i.e., the proposed index was successful in predicting flashover in about 82.3% of the overall physical flashover cases. This reveals the robustness of the proposed $R_{3/5}$% diagnostic index.

Results shown in Fig. 16 indicate that the EFS has a direct correlation with the level of pollution. As the level of pollution, represented by the pollution layer thickness, increases, the EFS also increases. Table IX shows that the EFS increases when the pollution thickness or conductivity increases, however, it decreases at high humidity levels. This effect agrees with the trend observed in the LC analysis when the value of $R_{3/5}$% decreases at a high humidity level (91%) compared to a lower humidity level (85%).

V. Real-Time Application Of The Proposed Method

The proposed method has the potential to be implemented in real-time to detect incipient degradation in the overhead insulators and thus avoiding potential consequences of sudden failures (see flowchart in Fig. 18).

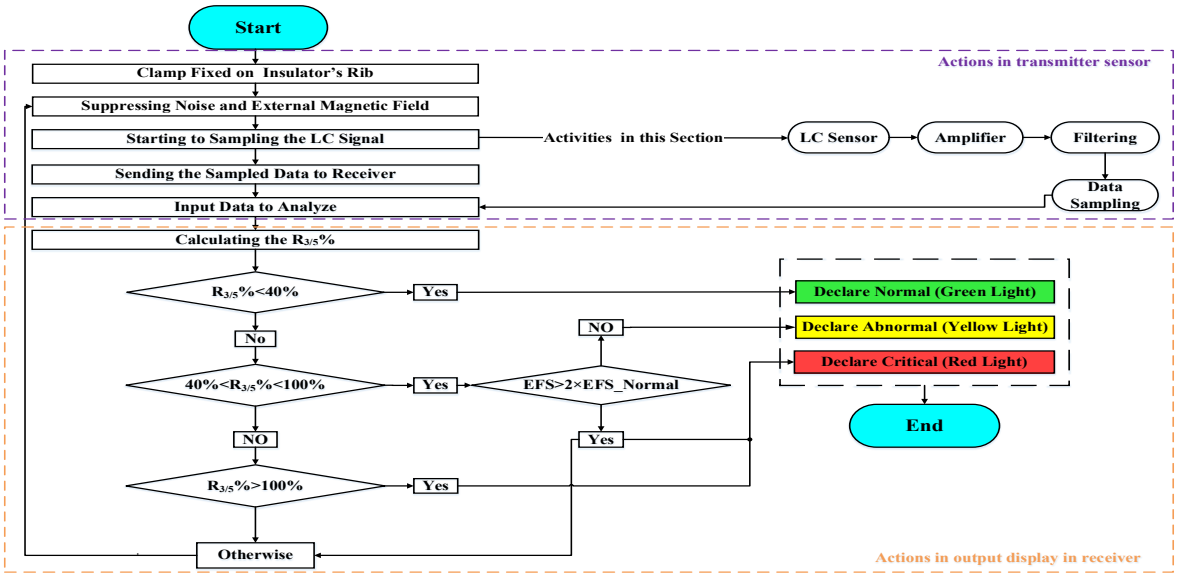

Fig. 18. Flowchart for the real-time implementation of the proposed diagnostic method.

In particular, the proposed online method can be used for wood poles in the vicinity of vegetation that are prone to bushfire due to power line failures, insulator degradation, and termite activity [30, 31]. The LC signal of in-field overhead line insulators can be measured using LC clamped sensor. Measured data can be sampled and transferred to a control center at which it can be analyzed to calculate the proposed index. The calculated index identifies the normal and critical state of the insulator. In case the index value is within the critical range as stated above, a complementary analysis using the insulator EFS is to be conducted using currently available commercial cameras or through monitoring corona discharge. The proposed real-time insulator monitoring process is shown in Fig. 18. In this figure, the composite insulator is considered normal if the value of $R_{3/5}$% is less than 40% whereas it is considered in critical condition if the proposed index is within the range 40%<$R_{3/5}$%<100% and the value of EFS is more than two times the value during normal condition. The insulator is considered in a significant critical condition when $R_{3/5}$% is more than 100%. It is to be noted that EFS is only used to quantify the criticality level of the investigated insulator. Hence, for real-time applications, only the value of $R_{3/5}$% is required to classify the condition of the insulator and identify a proper and timely asset management decision.

VI. Conclusion

The performance of the composite insulators in presence of pollution and humidity conditions is investigated to propose a reliable method to predict incipient flashover occurrence. Experimental tests are conducted to measure the LC signals of various insulators under different operating and pollution conditions. The harmonic spectra of the LC waveforms and the EFS and EP obtained using finite element simulation, are analyzed. The following conclusions can be drawn from the obtained results:

The harmonic spectrum of the LC signal is dominated by the 3rd and 5th harmonic components. However, similar to the THD, these components cannot be employed individually to identify and quantify the insulator condition, as they do not have a consistent trend. Results show that the percentage ratio of the two components, $R_{3/5}$%, has a consistent correlation with the insulator state, and hence it is of a good potential to predict the flashover occurrence. This indicator is proposed to be used along with the electric field distribution analysis to quantify the insulator health condition. The proposed method is easy to be employed in real-time with minimum measured parameters to develop an online condition-based monitoring system for the insulators of overhead lines. The proposed method can be applied for other insulator types; however, further research is required to identify its operational constraints. Also, further research on the measurements accuracy and uncertainty of the obtained data is recommended.

References

[1] M. F. Palangar, M. Mirzaie, A. Mahmoudi, "Improved flashover mathematical model of polluted insulators: A dynamic analysis of the electric arc parameters," *Electric Power Systems Research,* vol. 179, 2020, https://doi.org/10.1016/j.epsr.2019.106083.

[2] M. F. Palangar and M. Mirzaie, "Designation of an Indicator for flashover prediction of porcelain and glass insulators based on experimental tests", *Journal of Operation and Automation in Power Engineering*, vol. 3, no. 2, pp. 1691-1698, 2014.

[3] D. Pylarinos, K. Siderakis, and E. Pyrgioti, "Measuring and Analyzing Leakage Current Outdoor Insulators and Specimens", *Rev.Adv.Mater.Sci*., vol. 29, pp.31-53, 2011.

[4] E. Fontana, S. C. Oliveira, F. J. M. M. Cavalcanti, R. B. Lima, J. F. Martins-Filho, and E. Meneses-Pacheco, "Novel sensor system for leakage current detection on insulator strings of overhead transmission lines," *IEEE Transactions on Power Delivery,* vol. 21, no. 4, pp. 2064-2070, 2006.

[5] K. Li *et al.*, "A Novel Fault Leakage Current Detection Method With Protection Deadzone Elimination," *IEEE Transactions on Instrumentation and Measurement,* vol. 70, pp. 1-9, 2021.

[6] S. C. Oliveira and E. Fontana, "Optical Detection of Partial Discharges on Insulator Strings of High-Voltage Transmission Lines," *IEEE*

Transactions on Instrumentation and Measurement, vol. 58, no. 7, pp. 2328-2334, 2009.

[7]S. Oliveira and E. Fontana, "Optical system for flashover prediction in high voltage transmission lines", *Microwave and Optoelectronics Conference, 2007. IMOC 2007. SBMO/IEEE MTT-S International*, 2007, pp. 224-228.

[8]C. Volat, M. Jabbari, M. Farzaneh, and L. Duvillaret, "New method for in live-line detection of small defects in composite insulator based on electro-optic E-field sensor," *IEEE Transactions on Dielectrics and Electrical Insulation,* vol. 20, no. 1, pp. 194-201, 2013.

[9]M. M. Hussain, S. Farokhi, S. G. McMeekin and M. Farzaneh, "Dry band formation on HV insulators polluted with different salt mixtures," *2015 IEEE Conference on Electrical Insulation and Dielectric Phenomena (CEIDP)*, Ann Arbor, MI, USA, 2015, pp. 201-204.

[10] L. Zhengfa *et al.*, "Study on leakage current characteristics and influence factors of 110kV polluted composite insulators," in *2018 12th International Conference on the Properties and Applications of Dielectric Materials (ICPADM)*, 2018, pp. 896-900.

[11] M. Bi, Z. Yang, T. Jiang, X. Chen, and Y. Wang, "Study on Flashover Characteristic and Critical Flashover Current of icing and polluted 110kV Composite Insulators," in *2018 IEEE International Conference on High Voltage Engineering and Application (ICHVE)*, 2018, pp. 1-4.

[12] A. Kumar, A. R. Verma, and B. S. Reddy, "Leakage Current Analysis on Outdoor Composite Insulators," in *2020 IEEE International Conference on Computing, Power and Communication Technologies (GUCON)*, 2020, pp. 682-686.

[13] Y. Li, Z. Jia, and X. Wang, "Study on the interface between core and sheath of composite insulator based on leakage current," in *2018 12th International Conference on the Properties and Applications of Dielectric Materials (ICPADM)*, 2018, pp. 1127-1130.

[14] M. F. Palangar and M. Mirzaie, "Predicting Critical Conditions in Polluted Insulators Using Phase Angle Index of Leakage Current," in *2020 IEEE International Conference on High Voltage Engineering and Application (ICHVE)*, 2020, pp. 1-4.

[15] M. F. Palangar, M. Mirzaie, and M. F. Palangar, "Detecting of unnormal conditions of polluted insulators based on the analysis phase angle of leakage current," in *2015 20th Conference on Electrical Power Distribution Networks Conference (EPDC)*, 2015, pp. 7-15.

[16] M. F. Palangar, and M. Mirzaie, " Diagnosis of porcelain and glass insulators conditions using phase angle index based on experimental tests", *IEEE Transactions on Dielectrics and Electrical Insulation,* vol. 23, No. 3, pp. 1460-1466, 2016.

[17] M. F. Palangar, and M. Mirzaie, " Detection of critical conditions in ceramic insulators based on harmonic analysis of leakage current", *Electric Power Components and Systems,* vol. 44, No. 16, pp. 1854-1864, 2016.

[18] H. H. Kordkheili, H. Abravesh, M. Tabasi, M. Dakhem, and M. M. Abravesh, "Determining the probability of flashover occurrence in composite insulators by using leakage current harmonic components," *IEEE Transactions on Dielectrics and Electrical Insulation,* vol. 17, no. 2, pp. 502-512, 2010.

[19] H. Ha, S. Han, and J. Lee, "Fault Detection on Transmission Lines Using a Microphone Array and an Infrared Thermal Imaging Camera," *IEEE Transactions on Instrumentation and Measurement,* vol. 61, no. 1, pp. 267-275, 2012.

[20] J. Y. Kyu-Chil. Park, "Analyses of the Insulators' Radiation Noises for Error Detections," *Proceedings of Symposium on Ultrasonic Electronics,* vol. 30, p. 2, 18-20 November 2009.

[21] K. C. Park, Y. Motai, and J. R. Yoon, "Acoustic Fault Detection Technique for High-Power Insulators," *IEEE Transactions on Industrial Electronics,* vol. 64, no. 12, pp. 9699-9708, 2017.

[22] A. K. Upadhyay, P. Johri, C. C. Reddy, and A. Sandhu, "Direct Measurement of Accumulated Space Charge Using External Currents," *IEEE Transactions on Instrumentation and Measurement,* vol. 70, pp. 1-8, 2021.

[23] B. Wang et al., "Automatic Fault Diagnosis of Infrared Insulator Images Based on Image Instance Segmentation and Temperature Analysis," *IEEE Transactions on Instrumentation and Measurement*, vol. 69, no. 8, pp. 5345-5355, Aug. 2020.

[24] L. Jin, Z. Tian, J. Ai, Y. Zhang, and K. Gao, "Condition Evaluation of the Contaminated Insulators by Visible Light Images Assisted With Infrared Information," *IEEE Transactions on Instrumentation and Measurement*, vol. 67, no. 6, pp. 1349-1358, June 2018.

[25] N. N. Qaddoumi, A. H. El-Hag, and Y. Saker, "Outdoor Insulators Testing Using Artificial Neural Network-Based Near-Field Microwave Technique," *IEEE Transactions on Instrumentation and Measurement*, vol. 63, no. 2, pp. 260-266, Feb. 2014.

[26] E. Fontana et al., "Sensor Network for Monitoring the State of Pollution of High-Voltage Insulators Via Satellite," in IEEE Transactions on Power Delivery, vol. 27, no. 2, pp. 953-962, April 2012, DOI: 10.1109/TPWRD.2012.2183623.

[27] L. H. S. Silva, S. C. Oliveira, R. A. de Lima, and E. Fontana, "Long term analysis of leakage current pulses registered by an optical sensor network," 2013 SBMO/IEEE MTT-S International Microwave & Optoelectronics Conference (IMOC), 2013, pp. 1-5, DOI: 10.1109/IMOC.2013.6646584.

[28] D. Sadykova, D. Pernebayeva, M. Bagheri, and A. James, "IN-YOLO: Real-Time Detection of Outdoor High Voltage Insulators Using UAV Imaging," *IEEE Transactions on Power Delivery*, vol. 35, no. 3, pp. 1599-1601, 2020.

[29] M. Faramarzi Palangar, S. Mohseni, M. Mirzaie, and A. Mahmoudi, "Designing an Automatic Detector Device to Diagnose Insulator State on Overhead Distribution lines," in IEEE Transactions on Industrial Informatics, DOI: 10.1109/TII.2021.3073685.

[30] Abu-Siada, Ahmed; Mosaad, Mohamed I.; Mir, Saif: 'Voltage–current technique to identify fault location within long transmission lines', IET Generation, Transmission & Distribution, 2020, 14, (23), p. 5588-5596.

[31] A. Abu-Siada, Saif Mir, “A new on-line technique to identify fault location within long transmission lines”, Engineering Failure Analysis, Vol 105, Nov 2019, pp. 52-64.